Evidence for microbial iron reduction in the methanogenic sediments of the oligotrophic SE Mediterranean continental shelf

Hanni Vigderovich[1], Lewen Liang[2], Barak Herut[3], Fengping Wang[2], Eyal Wurgaft[1,4], Maxim Rubin-Blum[3] and Orit Sivan[1]

[1]The Department of Geological and Environmental Sciences, Ben-Gurion University of the Negev, Beer-Sheva, 8410501, Israel.
[2] School of Life Sciences and Biotechnology, Shanghai JiaoTong University, Shanghai, 200240, P.R.China.
[3] Israel Oceanographic and Limnological Research, Haifa, 31080, Israel.
[4]Currently: The Department of Marine Chemistry and Biochemistry, Woods-Hole Oceanographic Institution, Woods-Hole, USA
Correspondence to: Orit Sivan (oritsi@bgu.ac.il)

Abstract. Dissimilatory iron reduction is probably one of the earliest metabolisms, which still participates in important biogeochemical cycles such as carbon and sulfur. Traditionally, this process is thought to be limited to the shallow part of the sediment column, as one of the energetically favorable anaerobic microbial respiration cascade, usually coupled to the oxidation of organic matter. However, in the last decade iron reduction has been observed in the methanogenic depth in many aquatic sediments, suggesting a link between the iron and the methane cycles. Yet, the mechanistic nature of this link has yet to be established, and has not been studied in oligotrophic shallow marine sediments. In this study we present first geochemical and molecular evidences for microbial iron reduction in the methanogenic depth of the oligotrophic Southern Eastern (SE) Mediterranean continental shelf. Geochemical pore-water profiles indicate iron reduction in two zones, the traditional zone in the upper part of the sediment cores and a deeper second zone located in the enhanced methane concentration layer. Results from a slurry incubation experiment indicate that the iron reduction is microbial. The Geochemical data, Spearman correlation between microbial abundance and iron concentration, as well as the qPCR analysis of the mcrA gene point to several potential microorganisms that could be involved in this iron reduction via three potential pathways: H_2/organic matter oxidation, an active sulfur cycle or iron driven anaerobic oxidation of methane.

1 Introduction

Iron (Fe) is the fourth most abundant element in the Earth's crust. It appears as elemental Fe, Fe(II) and Fe(III), and has an important geobiological role in natural systems (Roden, 2006). Dissimilatory microbial iron reduction is likely one of the first evolutionary metabolisms, and plays a key role in the reductive dissolution of Fe(III) minerals in the natural environment (Weber et al., 2006), in the mineralization of organic matter in freshwater sediments (Roden and Wetzel, 2002), and as a redox wheel that drives the biogeochemical cycles of carbon, nitrogen, sulfur and phosphorous (Li et al., 2012).

Dissimilatory iron reduction is part of the anaerobic respiration cascade, in which different organic substrates are used for energy by microorganisms and oxidized to dissolved inorganic carbon (DIC). This is accomplished by reduction of electron acceptors, other than oxygen, according to their availability and

41 energy yield. Denitrification is the first respiratory process in anoxic sediments, followed by manganese
42 and iron reduction and then sulfate reduction. Methane (CH_4) production (methanogenesis) by archaeal
43 methanogens is traditionally considered to be the terminal process of microbial organic matter
44 mineralization in anoxic environments, after the other electron acceptors have been exhausted (Froelich
45 et al., 1979). When outward diffusing methane meets an electron acceptor it can be consumed by
46 microbial oxidation (methanotrophy). In anoxic marine sediments anaerobic oxidation of methane
47 (AOM) is coupled mainly to sulfate reduction (Hoehler et al., 1994). This process was found to consume
48 up to 90 % of the methane that diffuses upwards to the sulfate methane transition zone (SMTZ)
49 (Valentine, 2002).

50 The classical process of dissimilatory iron reduction is coupled to the oxidation of organic matter
51 (organoclastic iron oxidation, Eq. 1) (Lovley, 1991; Lovley et al., 1996). However, iron reduction can be
52 coupled to other processes as well, such as hydrogen (H_2) oxidation (hydrogenotrophic iron reduction)
53 (Eq. 1). Besides H_2 oxidation, Fe(III) can be reduced microbially (and also abiotically) by pyrite
54 oxidation (Eq. 2) (Bottrell et al., 2000), leading to S intermediates, and followed by their
55 disproportionation to sulfate and sulfide via a "cryptic" sulfur cycle (e.g. Holmkvist et al., 2011).

$$Fe^{3+} + organic\ matter/H_2/humic\ acids \rightarrow Fe^{2+} + HCO_3^-/CO_2 \tag{1}$$

$$FeS_2 + 14Fe^{3+} + 8H_2O \rightarrow 15Fe^{2+} + 2SO_4^{2-} + 16H^+ \tag{2}$$
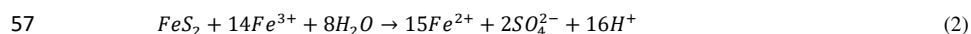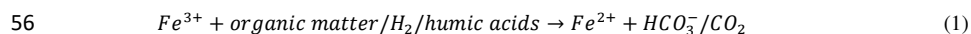
58 Another, recently discovered, pathway of iron reduction is by AOM (Eq. 3).

$$CH_4 + 8Fe(OH)_3 + 15H^+ \rightarrow HCO_3^- + 8Fe^{2+} + 21H_2O \tag{3}$$
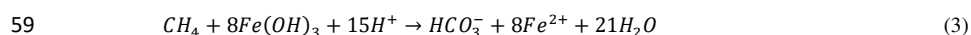
60 This process in marine sediments was evident through incubations of marine seeps (Beal et al., 2009;
61 Sivan et al., 2014). It was suggested through the modeling of geochemical profiles in deep sea sediments
62 (Sivan et al., 2007; Riedinger et al., 2014) and in brackish coastal sediments (Slomp et al., 2013; Segarra
63 et al., 2013; Egger et al., 2015; Egger et al., 2016; Rooze et al.,2016). In freshwater, it was suggested to
64 occur in lakes (Crowe et al. 2011; Norði et al., 2013), and was shown in enriched, denitrifying cultures
65 from sewage, where it was performed by methanogens (Ettwig et al., 2016). Iron-coupled AOM in natural
66 lake sediments was indicated using isotope pore-water depth profiles (Sivan et al., 2011), rate modeling
67 based on these profiles (Adler et al., 2011), microbial profiles (Bar-Or et al., 2015), and directly by a set
68 of sediment slurry incubation experiments using several methods (Bar-Or et al. 2017). The few microbial
69 studies about iron-coupled AOM (mainly in cultures) showed the involvement of
70 methanogenic/methanotrophic archaea (Scheller et al., 2016; Ettwig et al., 2016; Cai et al., 2018; Yan et
71 al., 2018; Rotaru and Thamdrup, 2016) or cooperation between methanotrophic archaea and iron
72 reducing bacteria (Bar-Or et al., 2017).

73 Whereas Fe(II) is highly soluble, Fe(III) appears as low solubility minerals, and is the most abundant
74 species of iron under natural conditions close to neutral pH. This makes iron usage a challenge to
75 microorganisms, which need to respire low-solubility iron oxide minerals, thus rendering many of iron-
76 oxide minerals effectively unavailable for reduction and leading to the dominance of sulfate reducing
77 bacteria beyond a certain depth.

78 Therefore, the observation of iron reduction below its traditional depth, in the methanogenic zone, where
79 iron-oxides are assumed to be inactive, is surprising. Moreover, this reduction is occasionally
80 accompanied by a depletion in methane concentrations, suggesting a possible link between the iron and
81 the methane cycles. The coupling can be through a competition between methanogens and iron reducing
82 bacteria, methanogens switching from methanogenesis to iron reduction metabolism, and/or iron coupled
83 AOM, as mentioned above. Previous observations in other environments demonstrated the inhibition of
84 methanogenesis under iron-reducing conditions due to competition between methanogens and iron-
85 reducing bacteria for the common acetate and hydrogen substrates (Conrad, 1999; Lovley and Phillips,
86 1986; Roden and Wetzel, 1996; Roden, 2003). Different methanogens can also utilize iron directly, by
87 reducing Fe(III). This was shown in pure cultures with the amorphous Fe(III) oxyhydroxide (Bond and
88 Lovley., 2002), in pure cultures close to natural sedimentary conditions (Sivan et al., 2016), in natural
89 lake sediments with different iron oxides (i.e. amorphous iron, goethite, hematite and magnetite) (Bar-or
90 et al., 2017), and in iron-rich clays (Liu et al., 2011; Zhang et al., 2012; Zhang et al., 2013).

91 Despite the above studies, the nature of the link between the iron and the methane cycles in marine
92 methanogenic zone, which reactivates iron oxides and making them available for reduction, has not been
93 determined yet. Furthermore, microbial iron reduction in methanogenic zones has not been shown in
94 oligotrophic shallow marine environments. In this study we report observations of microbial iron
95 reduction in the methanogenic depth in marine sediments of the oligotrophic SE Mediterranean
96 continental shelf. We show both geochemical pore-water profiles and microbial investigation at three
97 different stations combined with a basic incubation experiment with slurry from the methanogenic zone.
98 These profiles and the incubation, including the related microorganisms, are discussed in terms of the
99 possible links between iron and methane cycles.

100 **2 Methods**

101 **2.1 Study site**

102 The Levantine Basin of the SE Mediterranean Sea is one of the most oligotrophic nutrient-poor marine
103 environment in the world (Kress and Herut, 2001), including the Israeli continental shelf (Herut et al.,
104 2000). The continental shelf narrows from south to north and is built mainly of Pliocene-Quaternary
105 Nile-derived sediments, whose rate of sedimentation decreases with increasing distance from the Nile
106 Delta and from the shoreline (Nir, 1984; Sandler and Herut, 2000). While the highest levels of total
107 organic carbon (TOC) (1 – 2%) in sediments were found in the Western Mediterranean Basin and
108 offshore the Nile River delta, the central and eastern deep water regions of the Levantine Basin have
109 relatively low TOC levels (0 – 0.5%) (Astrahan et al., 2017). Along the Egyptian coast, maximal contents
110 of TOC in surface sediments on the shelf is up to 1.5% (Aly Salem et al., 2013), while in the Israeli shelf
111 sediments (< 100 m depth) the TOC levels vary between < 0.1 – 1% (Almogi-Labin et al., 2009). The
112 discovery of a 'gas front' from seismic profiles within the sediments of the continental shelf of Israel
113 (Schattner et al., 2012), led to the findings of biogenic methane formation at some locations in shallow
114 sediments (Sela-Adler et al., 2015). The bottom seawater across the shelf is well oxygenated therefore
115 sulfate concentration in the water-sediment interface is ~30 mmol L^{-1} (Sela-Adler et al., 2015).

2.2 Sampling

Seven sediment cores (~5 – 6 m long) were collected using a Benthos 2175 piston corer, from the undisturbed seafloor sediments of the SE Mediterranean continental shelf of Israel at water depths of 81 – 88 m from three stations; SG-1 (32°57.82' N 34°55.30' E), PC-3 (32°55.30' N 34°54.14' E) and PC-5 (32°55.47' N 34°55.01' E). The cores were sampled by the R.V. *Shikmona* between 2013 to 2017, and by the R.V. *Bat-Galim* on January 2017. The sediment cores were sliced on board every 25 – 35 cm within minutes upon retrieval from the seafloor. These stations were investigated previously with other focuses, such as the sulfate reduction in the SMTZ (Antler et al., 2015; Wurgaft et al., unpublished), and methanogenesis characteristics (Sela-Adler et al., 2015).

From each interval, a 2.5 mL sediment sample was collected and inserted into an anaerobic 10 mL glass bottle filled with 5 mL NaOH 1.5 N for headspace measurements of methane concentration (after Nusslein et al, 2003). In addition, another 2.5 mL sediment sample was taken from each segment of the cores and transferred into a 20 mL glass bottle filled with NaCl saturated solution for H_2 concentrations measurements. Sediment samples from each segment of the cores were centrifuged on board if possible or in the lab within a day by Sorval centrifuge at 9500 RPM under 4 °C and Ar atmosphere in order to extract pore-water for chemical analysis. The supernatant was filtered (0.22 µm) and analyzed for Fe(II), sulfate, sulfide and the isotope composition of the DIC ($\delta^{13}C_{DIC}$). After the pore-water extraction, the sediment was analyzed for the content of the different iron oxides. In addition, sediment sub-sample from each segment of the January 2017 core from SG-1 station was kept in -20 °C for molecular analysis. Due to high water content in the upper part of the sediments, the top 20 cm of the piston cores pore-water measurements might be affected by sediment movement and mixing; to avoid this, two ~30 cm cores were collected during the September 2015 and January 2017 cruises via a 0.0625 m^2 box corer (Ocean Instruments BX 700 Al). The cores were stored at 4 °C and cut in the lab less than 24 hours after their collection. Sediment and pore-water samples were measured for CH_4, Fe(II), sulfate and $\delta^{13}C_{DIC}$ measurements.

2.3 Slurry incubation experiment

The experimental set-up consisted of 11 bottles with sediment from the methanogenic zone, 260 cm below sea floor level from SG-1 station, where iron reduction was apparent in the pore-water profiles. The sediment from the designated depth was homogenized in an anaerobic bag under N_2 atmosphere. It was then transferred under anaerobic conditions to a 250 mL glass bottle with the addition of synthetic sea water without sulfate to reach 1:1 sediment – water slurry ratio for 3 months incubation period. Then the slurry was sub-divided anaerobically to the 60 mL experiment bottles, and synthetic sea water was added for final sediment – water ratio of 1:3. The bottles were sealed with a crimp cap and were flushed with N_2 for 5 minutes, shaken vigorously and flushed again, (repeated 3 times). The experiment bottles were amended with iron oxides (hematite (Fe_2O_3) or magnetite (Fe_3O_4) with final concentration of 10 mmol L^{-1}) with/without hydrogen (H_2) (to the final concentration of ~4% of the Head space volume). The experiment bottles were sampled several times for dissolved Fe(II) concentrations during the 14 day experiment period.

2.4 Analytical methods

2.4.1 Pore-water analyses

Methane concentrations were analyzed by Focus Gas – Chromatograph (GC; Thermo) equipped with FID detector with detection limit of 50 µmol L^{-1}. H$_2$ concentrations were analyzed in a Reducing Compound Photometer Gas-Chromatograph (RCP-GC; Peak Laboratories). Dissolved Fe(II) concentrations were measured using the ferrozine method (Stookey, 1970) by a spectrophotometer at 562 nm wavelength with detection limit of 1 µmol L^{-1}. Sulfide was measured using the Cline (1969) method by a spectrophotometer at 665 nm wavelength with detection limit of 1 µmol L^{-1}. Sulfate concentrations were measured in an inductive coupled plasma atomic emission spectrometer (ICP-AES), Perkin Almer Optima 3300, with an analytical error of ±1% (average deviations from repeated measurements of a seawater standard). The $\delta^{13}C_{DIC}$ values were measured on a DeltaV Advantage Thermo© isotope-ratio mass-spectrometer (IRMS) at a precision of ±0.1 ‰. Results are reported versus VPDB standard. Several pore-water profiles were performed during the study, and all of them are presented (and not their average). For each profile, the error bar is that of the average deviation of the mean of the duplicates, in cases where they were taken, otherwise it is that of the analytical error (if larger than the symbol).

2.4.2 Sediment analysis

Reactive Fe(III) in the sediments was measured according to Poulton and Canfield (2005) definition and sequential extraction procedure. The different reactive iron oxides were separated to (1) carbonate-associated Fe; (2) easily reducible oxides; (3) reducible oxides and (4) magnetite. At the end of each extraction stage, the extractant was transferred to a 15 mL falcon tube with 0.1 mL ascorbic acid and 0.1 mL ferrozine solution to reduce all the Fe(III) to Fe(II) and fix it, then it was measured spectrophotometrically. The results are presented as "reactive Fe(III)", which was the sum of the easily reducible oxides, reducible oxides and magnetite.

2.4.3 Quantitative PCR and 16S rRNA gene V4 amplicon pyrosequencing

DNA was extracted from the sediment core of station SG-1 from January 2017 using PowerSoil DNA Kit (MoBio Laboratories, Inc., Carlsbad, CA, USA) following manufacturer's instructions. Copy numbers of selected genes were estimated with quantitative PCR (qPCR) as described previously (Niu et al., 2017) using specific primers: Uni519f/Arc908R and bac341f/519r for archaeal and bacterial 16S rRNA genes, respectively, and mlas/mcrA-rev for the *mcrA* gene, which encodes the α-subunit of methyl-coenzyme M reductase. The amplification efficiency was 94.5%, 106.3% and 92.4% for the archaeal 16S rRNA, bacterial 16S rRNA and the *mcrA* gene, respectively (the respective R^2 of the standard curve was 0.998, 0.998 and 0.995).

The V4 regions of bacterial and archaeal 16S rRNA genes were amplified using barcoded 515FB/806RB primers (Walters et al., 2015) and Arch519/Arch806 primers (Song et al., 2013), respectively. PCR mixture contained 6 – 10 ng total DNA, 5 µL 10× Ex Taq buffer, 4 µL 2.5 mmol L^{-1} dNTP mix, 1 µL of each primer, 0.25 µL Ex Taq polymerase (Ex-Taq; TaKaRa, Dalian, China) and 5 µL bovine serum albumin (25 mg mL^{-1}) in a total volume of 50 µL. DNA was sequenced as 2x150 bp reads using Illumina MiSeq platform (Illumina, USA). Sequence quality assessments, chimera detection and down-stream

192   phylogenetic analyses were conducted in QIIME (Caporaso et al., 2010). Taxonomical assignments for

193   each OTU were performed in QIIME using the BLAST method and the SILVA128 reference database.

194   24056 to 132042 high quality sequences were obtained per sample, with the proportion of high-quality

195   sequence versus total sequence between 81.97 – 99.89%. Spearman correlation was performed using the

196   online calculator (http://www.sthda.com/english/rsthda/correlation.php) to test the relevance of

197   microbial abundance and communities with Fe(II) concentration along the depth of the sediment core

198   from 185 cm to the bottom 575 cm, which is the methanogenic zone of the sediment core according to

199   the geochemical profile (see the results below).

200   **3 Results**

201   **3.1 Geochemical profiles**

202   Geochemical pore-water profiles of several sediment cores from the three stations (SG-1, PC-3 and PC-

203   5) were performed in order to test the possibility of the iron reduction process in the methanogenic zone

204   of the SE Mediterranean continental shelf and its potential sources. Pore-water analyses of sulfate

205   concentrations show complete depletion at approximately 150 cm depth in all cores at station SG-1 (Fig.

206   1). Sulfide concentrations were below the detection limit in all cores and therefore are not presented.

207   Methane profiles show an increase in concentration immediately after the consumption of sulfate. The

208   maximal methane concentration was the saturation level (Sela-Adler et al., 2015) of about 10 mmol L^{-1}

209   at ~140 cm depth in June 2015 (station SG-1), probably due to intensive methane production at the exact

210   location of the core collected at that time. The other methane depth-profiles show high concentrations of

211   methane of approximately 2 mmol L^{-1} all the way to the bottom of the cores (~600 cm). Detected

212   dissolved Fe(II) concentrations were found in the traditional iron reduction zone in the upper part of the

213   cores (between 30 – 90 cm depth). However, a second peak was found in the deeper part of the sediment,

214   at the methanogenic zone (below 180 cm depth). Maximum dissolved Fe(II) concentrations reached 84

215   μmol L^{-1} in the traditional iron reduction zone of the sediment cores, and 65 μmol L^{-1} in the methanogenic

216   zone (Fig. 1). It should be noted that iron species are highly sensitive to environmental changes such as

217   shifts in local pH, the different types of electron shuttles, and organic compounds that are present in the

218   surroundings. These changes affect the net dissolved Fe(II) observed; consequently the dissolved Fe(II)

219   results show variability between the cores that were extracted and analyzed from the same station. The

220    $\delta^{13}C_{DIC}$ values were the lowest (-35 ‰) at the SMTZ depth, as expected from the intensive sulfate-

221   coupled AOM process there, which uses the isotopically light carbon of the methane as a carbon source

222   with only small fractionation. The $\delta^{13}C_{DIC}$ values were the highest in the methanogenic zone, as expected

223   (the carbon source for the methane comes from the CO_2, leaving the residual DIC heavier by about 60

224   ‰ (Whiticar, 1999)). Fitting the intensive methane profile from June 2015, the $\delta^{13}C_{DIC}$ showed the most

225   dramatic decrease and increase that date as well. The SMTZ was also the shallowest in this core because

226   of the intensive methane oxidation, thus the traditional iron reduction is missing in the sampled pore-

227   water. H_2 concentrations decreased to a minimum peak of 17 nmol L^{-1} at 155 cm depth, and then

228   increased to a maximum of 147 nmol L^{-1} at 485 cm depth.

229   Pore-water analyses from station PC-3 on all three sampling dates show similar patterns to SG-1 with

230   less methane activity (Fig 1). Sulfate was completely depleted within the upper 300 cm depth. Sulfide

231   concentrations were below the detection limit at this station as well. The methane profiles show an

232   increase in methane concentration immediately after the consumption of sulfate. The maximum methane

233   concentration reached 0.8 mmol L^{-1} at 450 cm depth in the Aug-13 core. Fe(II) profiles show two peaks,

234   one in the upper part of the cores with maximum of 32 µmol L^{-1} at 177 cm depth, and another one with

235   maximum of 64 µmol L^{-1} at 390 cm depth at the methanogenic depth. The $\delta^{13}C_{DIC}$ decreased from

236   approximately -10 ‰ at the water-sediment interface to -20 ‰ at the SMTZ. Below that zone there was

237   an increase in $\delta^{13}C_{DIC}$ values to about -5 ‰ due to methanogenesis. H_2 concentrations remained around

238   2 µmol L^{-1} along the core. The few deviating points do not fit a clear pattern and therefore not discussed.

239   The H_2 concentrations at the PC-3 station are higher by one order of magnitude than the concentrations

240   at the SG-1 station. This is probably due to the more intensive methanogenesis process at SG-1 station,

241   as shown by the higher methane concentrations than those at PC-3 station.

242   Pore-water analyses from the core collected at station PC-5 resembles the profiles of PC-3 station. Sulfate

243   was depleted at approximately 300 cm, and methane concentrations increased below that depth to 0.3

244   mmol L^{-1}. The Fe(II) profile shows two peaks in this core as well, one in the upper part of 20 µM at 150

245   cm depth and the second of 30 µmol L^{-1} in the methanogenic zone. The $\delta^{13}C_{DIC}$ value decreased from -5

246   ‰ at the water-sediment interface to -25 ‰ at the SMTZ, and below that depth $\delta^{13}C$ values increased to

247   -17 ‰.

248   The reactive Fe(III) oxide profile from SG-1 (Fig. S1) shows a general decrease from 3 dry wt % at 13

249   cm depth to 2.3 dry wt % at 507 cm depth, with two minimum peaks of 2.4 dry wt % at 103 cm and of

250   1.9 dry wt % at 312 cm. PC-3 profile shows no significant trends in the reactive Fe(III) concentrations.

251   The values vary between 2.1 dry wt %, which is the maximum point at 167 cm, and 1.8 dry wt %, which

252   is the minimum point at 137 cm depth.

253   **3.2 Abundance and diversity of bacteria and archaea**

254   The qPCR of bacterial and archaeal 16S rRNA genes from the SG-1 core revealed that the abundance of

255   bacterial genes was between $1.46 - 9.45 \times 10^6$ copies per g wet sediment, while that of archaea was

256   between $8.15 \times 10^5 - 2.25 \times 10^7$ copies per g wet sediment (Fig. 2). These abundances are typical to

257   oligotrophic marine sediments (e.g. South China Sea that contain ~0.5 – 1 % TOC (Yu et al., 2018a).

258   The abundance of bacteria and archaea decreased gradually in the top 95 cm, increased sharply at 125

259   cm within the SMTZ, remained relatively stable with high abundance at 185 – 245 cm (the top layer of

260   the methanogenic zone), and then decreased. Notably, the abundance of both bacteria and archaea peaked

261   within the methanogenic zone at 245 cm in correspondence with a Fe(II) concentration peak. However,

262   it is not feasible to compare the abundance of archaea and bacteria by this method due to bias caused by

263   the PCR primers used (Buongiorno et al., 2017). The abundance of the *mcrA* gene increased sharply from

264   the surface layer to the SMTZ, peaked at 155 cm and remained stable at 155 – 245 cm, indicative of

265   active anaerobic methane metabolism in the SMTZ and active methanogenic zone (Fig. 2). Spearman

266   correlation test shows that the abundance of the bacteria and archaea 16S rRNA genes and *mcrA* genes

correlated with Fe(II) concentration in the methanogenic zone, where *mcrA* gene correlated the most significantly (r = 0.5429, p value = 0.04789).

Illumina-sequencing of the 16S rRNA gene revealed diverse bacterial and archaeal communities throughout the SG-1 core. Although no clear plateau was observed on species rarefaction curve for the current sequencing depth (Fig. S2), Shannon diversity indices reached stable values, indicating that those sequences well covered the diversity of bacterial and archaeal populations in the samples (Fig. S3). Shannon index, based on 16S rRNA gene sequences, showed higher diversity in the top layers of the sediment along with similar values through the core using the bacterial primers, while for sequences using archaeal primers, the values varied in different layers (Table S1). The bacterial sequences were affiliated with the following phyla: Planctomycetes (25.7%), Chloroflexi (23.2 %), Proteobacteria (12.9%), Deinococcus-Thermus (9.9 %), Acidobacteria (3.5%), Aminicenantes (3.3 %), Spirochaetes (2.3%), Deferribacteres (1.7%), Elusimicrobia (1.6%), Aerophobetes (1.6%), Nitrospirae (1.4%), Firmicutes (1.4 %), Actinobacteria (1.4 %), TM6 (Dependentiae) (1.2%), Marinimicrobia (SAR406 clade) (1.0%), and other taxa with less than 1% of the bacterial communities (Fig. 3a). Bathyarchaeota were the predominant archaea in all the sediment layers, based on the high relative abundance of their 16S rRNA gene sequences (91.0%). The remaining archaeal phyla comprised Euryarchaeota (3.2%), Thaumarchaeota (2.4%), Lokiarchaeota (1.0%), and other phyla with less than 1% of the archaeal communities (Fig. 3b). Spearman correlation analysis revealed that uncultured SBR1093 (r = 0.6176, p value = 0.01859) from bacterial Candidate Phylum SBR1093, subgroup 26 of Acidobacteria (r = 0.5841, p value = 0.02828), the uncultured bacterium from TK10 Class of Chloroflexi phylum (r = 0.5297, p value = 0.0544) and *uncultured Bathyarchaeota sp.* (archaea) (r = 0.5516, p value = 0.04388) correlated significantly with Fe(II) iron concentration.

3.3 Incubation experiment

Sediment from the observed deep iron reduction zone of SG-1 station from January 2017 core was taken for a basic short-term (few weeks) slurry incubation experiment in order to characterize the iron reduction process in the methanogenic zone. The results of the experiment are shown in figure 4. Dissolved Fe(II) concentrations show significant increase from 11 μmol L^{-1} to approximately 90 μmol L^{-1} during the first three days in all the experimental bottles, except for the killed bottles, implying that the reduction is microbially mediated. Another observation was that the microorganisms were able to reduce both hematite and magnetite to the same extent. In addition, no difference in the Fe(II) concentrations between bottles with and without the addition of H$_2$ was observed.

4 Discussion

This study was performed in the SE Mediterranean in the area of the recently discovered 'gas front' (Schattner et al., 2012), where biogenic methane was found at some locations in shallow sediments with low TOC content (Sela-Adler et al., 2015). SG station is located at the center of this area, while PC-3 and PC-5 at the edges, and indeed methane involved processes seem more intensive at this station (SG-1) (Fig. 1). At this station methane reaches higher concentrations, and the intensive methanogenesis also leads to intensive methane oxidation by sulfate at the SMTZ, causing it to occur at shallower depth with

305   lower $\delta^{13}C_{DIC}$ values, as observed in previuos studies (e.g. Sivan et al., 2007). The shallower SMTZ

306   values also interfered with the ability to observe the traditional iron reduction zone in our SG-1 sampling

307   resolution.

308   Despite the pore-water profiles variability between the stations, they show a resemblance in their trends.

309   All geochemical pore-water and reactive Fe(III) profiles suggest that the sediments in this area of the SE

310   Mediterranean shelf can be classified into three general depth-zones (Fig. 1): **zone 1** is the upper part of

311   the sediment, where the traditional classical iron reduction occurs, probably coupled to organic matter

312   oxidation, with sulfate reduction below it; **zone 2** is the SMTZ, where methane starts to increase with

313   depth, sulfate is completely depleted, sulfide is absent and Fe(II) is either present in low concentrations

314   or absent as well (probably due to the precipitation of iron-sulfide minerals); **zone 3** is the methanogenic

315   zone, where methane concentrations increased to the highest values in all stations. At this zone, local

316   maxima of Fe(II) concentrations in the pore-water were found in all cores, indicating iron oxides

317   reactivation and reduction. The results of the slurry experiment show only a slight increase in Fe(II)

318   concentrations in the killed bottles compared to the non-killed bottles, indicating that most of the iron

319   reduction in zone 3 is microbial (Fig. 4).

320   The observed intensive iron reduction in the methanogenic sediments is the first in the Southeastern

321   Mediterranean shelf. The phenomenon of iron reduction in the methanogenic depth has been observed

322   before in other marine provinces (Egger et al., 2016; Jorgensen et al., 2004; März et al., 2008; Riedinger

323   et al., 2014; Slomp et al., 2013; Treude et al., 2014), however, the type of link to the methane cycle is

324   complex. Usually, iron reduction is coupled to oxidation of organic matter (Lovley and Phillips, 1988)

325   and is performed by iron reducing bacteria, which is probably the case in zone 1. It is however

326   questionable if this also stands for zone 3 and if not, what process is responsible for the reactivation of

327   iron oxides at this depth and its relation to methane.

328   The oligotrophic nature of the studied area would suggest that intensive bacterial iron reduction coupled

329   to the oxidation of organic matter in zone 3 is less likely. The present low nutrient and low chlorophyll

330   concentrations in the water results in low amount of TOC in the sediments, reaching up to ~1% (Sela-

331   Adler et al., 2015). However, we observe in situ biogenic methane formation in the shallow shelf

332   sediments based on the geochemical ($\delta^{13}C_{DIC}$) and microbial profiles (population and functional *mcrA*

333   gene). This indicates that regardless the area's present oligotrophic nature, the TOC substrate is enough

334   to sustain all the microbial activity up to methanogenesis. These environmental conditions are

335   hypothetically attributed to the Last Glacial Maximum or Mid-Pleistocene sources (Schattner et al.,

336   2012). At the methanogenic zone and below, it might be that the microbial communities present at these

337   depths are used as a food source.

338   Another potential process that can be coupled to iron reduction in the methanogenic zone is H_2 oxidation.

339   H_2 is an important intermediate in anaerobic aquatic sediments. In this type of environment, it is produced

340   mainly by fermentation of organic matter (Chen et al., 2006), and can be involved in different microbial

341   processes; where each process would need a certain amount of H_2 in order to occur (Lovley and Goodwin,

342   1988). The H_2 levels at stations SG-1 and PC-3 (Fig. 1) are relatively high (Lilley et al., 1982; Novelli et

343 al., 1987), suggesting that there is enough H_2 to sustain the iron reduction process. The increase in H_2

344 concentration at the methanogenic zone in SG-1 station could be explained by the occurrence of

345 fermentation processes, which enables H_2 to accumulate (Chen et al., 2006).

346 H_2 involvement was tested by injecting 1 mL of this gas to the experimental bottles in the methanogenic

347 iron reduction process (Fig. 4). We observed that the increase of Fe(II) concentration was similar in the

348 bottles with H_2 addition compared to the bottles without H_2. This could mean that either there is enough

349 H_2 in the sediments as it is, as implied by the H_2 pore-water profiles, or that at the methanogenic depth

350 H_2 is not involved in the iron reduction process.

351 A different way to reactivate the iron reduction process in zone 3 is to have an active sulfur cycle at this

352 depth. In this scenario, Fe(III) is reduced by pyrite oxidation (Eq. 3) (Bottrell et al., 2000), which triggers

353 the sulfur "cryptic" cycle (Holmkvist et al., 2011). In this cycle elemental sulfur and eventually, by

354 disproportionation, sulfide and sulfate are produced, the sulfide reacts with iron-oxide and precipitates

355 as FeS. The sulfate can inhibit methanogenesis (Mountfort et al., 1980; Mountfort and Asher, 1981),

356 which can result in the enhancement of the iron reduction process due to competition for substrate with

357 the methanogenesis process.

358 The recently discovered iron coupled AOM process (Eq. 3) is another potential process that involves iron

359 oxides reduction in the methanogenic zone. Fe(III) as an electron acceptor for AOM provides a greater

360 free energy yield than sulfate (Zehnder and Brock, 1980), and its global importance was emphasized

361 (Sivan et al., 2011; Lovley, 1991a; Kappler and Straub, 2005; Roden, 2003). In our profiles AOM could

362 be a valid option, as can be inferred from figure 5, where inverse association was observed between the

363 dissolved Fe(II) concentrations in zone 3 and the methane concentrations. In most cores presented in the

364 figure it is apparent that at high concentrations of Fe(II), methane concentrations are low (relatively to

365 the specific core), and at high methane concentrations, Fe(II) concentrations are low (relatively to the

366 specific core). This could be a result of iron-coupled AOM that uses methane to reduce Fe(III)-oxides,

367 releasing dissolved Fe(II) to the pore-water. This can also suggest a type of competitive relationship

368 between methanogenesis and microbial iron reduction; perhaps over substrate, or microbial population

369 switching from methanogenesis to iron reduction metabolism (e.g. Sivan et al., 2016). It should be noted

370 that our experiment was not designed to test AOM due to its short time scale of a few weeks, hence

371 another long experiment with the addition of the ^{13}C-labeled methane will enable us to shed more light

372 on this association.

373 Our data profiles and incubation indicate that iron reduction is performed and stimulated by microbial

374 activity. This is despite the fact that the known potential bacterial iron reducers, such as *Alicyclobacillus*,

375 *Sulfobacillusin*, *Desulfotomaculum* genera (Firmicutes), *Acidiphilium* (Alphaproteobacteria);

376 *Desulfobulbus*, *Desulfuromonas*, *Geobacter*, *Geothermobacter, Anaeromyxobacter* (Deltaproteobacteria)

377 and *Shewanella* (Gammaproteobacteria) (Weber et al., 2006) comprise less than 0.1% of bacteria

378 detected in the methanogenic zone (from 185 cm and below). This is because it appears that both the

379 microbial abundance and the Fe(II) concentration peaked at the methanogenic zone. Cultivation efforts

380 indicated that archaeal methanogens may also play a role in iron reduction within sediments (Sivan et al.,

381 2016). Moreover, the relative abundance of methane-metabolizing archaea was shown to correlate with
382 Fe(II) concentrations in Helgoland muds from the North Sea, where microbial abundance and the Fe(II)
383 concentrations peaked at the methanogenic zone, similarly to the Mediterranean sediments (Oni et al.,
384 2015). It is possible that methane-metabolizing archaea were involved in the iron reduction in the
385 Mediterranean sediments, as the highest *mcrA* gene copies per gram wet sediment were detected in the
386 SMTZ and in the top of the methanogenic zone where the Fe(II) concentrations are high. Methanotrophs,
387 such as ANMEs, were found to be involved in iron coupled AOM in marine and freshwater cultures
388 (Scheller et al., 2016; McGlynn et al., 2015; Ettwig et al., 2016; Cai et al., 2018). ANMEs were found
389 with relatively low frequencies (ANME1, below 1% in most samples, circa 5% in the 185 cm layer), and
390 their role in iron reduction within the Mediterranean sediments remains to be tested. It should be noted
391 that even though, the microbial population was tested only on the sediment core that was extracted on
392 January 2017 at SG-1 station, we believe that it represents the general microbial population abundance
393 in the SE Mediterranean continental shelf.

394 In our study, Spearman correlation analysis revealed that bacterial phyla SBR1093 (candidate Phylum),
395 Acidobacteria and Chloroflexi, as well as archaeal Phylum Bathyarchaeota showed significant
396 correlation with a Fe(II) concentration in the methanogenic zone. The Candidate Phylum SBR1093 was
397 firstly identified in phosphate-removing activated sludge from a sequencing batch reactor (Bond et al.,
398 1995), and continuously detected in a short-chain fatty acid rich environment such as wastewater
399 treatment, and marine sediments (Wang et al., 2014). It was thought to be capable of growing
400 autotrophically, but the metabolic capabilities related to iron reduction remain unclear. Strains of
401 Acidobacteria and Chloroflexi phylum were found to be capable of iron reduction (Kawaichi et al., 2013;
402 Kulichevskaya et al., 2014). In addition, members of Acidobacteria were found in iron-coupled AOM
403 enrichment (Beal et al., 2009). The metabolic properties of Subgroup 26 from Acidobacteria and TK10
404 Class of Chloroflexi are still not known. Bathyarchaeota are globally distributed and account for a
405 considerable fraction of the archaeal communities in the marine sediments, particularly, in the
406 Mediterranean Pleistocene sapropels (Coolen et al., 2002; Zhou et al., 2018). While Bathyarchaeota have
407 diverse metabolic capabilities (Lloyd et al., 2013; Meng et al., 2014; Evans et al., 2015; He et al., 2016;
408 Yu et al., 2018b; Feng et al., 2019), their role in iron reduction warrants further studies, as suggested
409 from their high abundance here. Therefore, iron reduction and methane cycling within the deep
410 methanogenic zone may be facilitated by an interplay among bacterial and archaeal groups, whose
411 physiology and functions needs further investigation.

412 The geochemical and microbial data from the profiles and the slurry incubation experiment suggest that
413 deep iron reduction is occurring in the methanogenesis depth, and that both Bacteria and archaea can be
414 involved in the process. The geochemical profiles show Fe(II) peaks in the deep part of the sediments,
415 indicating iron reduction. The iron reduction was shown also in the incubation experiment, where
416 microbial involvement was evident. The Spearman correlation pointed out several potential microbial
417 players (bacterial and archaeal) that correlate to the dissolved Fe(II) profiles (e.g. Bathyarchaeota,
418 Acidobacteria and Chloroflexi). The geochemical conditions lead to three possible microbial iron
419 reduction pathways: a) H_2 or organic carbon oxidation, b) an active sulfur cycle, or c) iron driven AOM.

420 To verify the main iron reduction process at the methanogenic depth of the Mediterranean shelf sediments

421 further incubations and microbial work are needed.

422 **5 Author contribution**

423 H.V and O.S designed research; B.H was the PI of the cruises and M.RB was part of the scientific crew

424 on the ship; H.V, E.W and L.L performed research and analyzed the data; H.V, O.S, B.H, F.W, M.RB

425 and L.L synthesized the data and wrote the paper.

426 The authors declare that they have no conflict of interest.

427 **6 Acknowledgments**

428 The authors thank the captain and craw of the R/V Shikmona and R/V Bat Galim from the Israel

429 Oceanographic and Limnological Research for all their help during field sampling. Many thanks to E.

430 Eliani-Russak for her technical assistance in the lab and to V. Boyko for her help with the reactive iron

431 speciation procedure. We also thank all of Orit's lab member for their help. This study was supported by

432 the joint grant of Israel Science Foundation and the National Natural Science Foundation of China (ISF-

433 NSFC) [grant number 31661143022 (FW) and 2561/16 (OS)]. Funding was provided to H. Vigderovich

434 by the Mediterranean Sea Research Center of Israel.

435

436 **References**

437 Adler, M., Eckert, W. and Sivan, O.: Quantifying rates of methanogenesis and methanotrophy in Lake

438 Kinneret sediments (Israel) using pore-water profiles, Limnol. Oceanogr., 56(4), 1525–1535,

439 doi:10.4319/lo.2011.56.4.1525, 2011.

440 Almogi-Labin, A., Herut, B., Sandler, A., Gelman, F.: Fast changes at the Israeli continental shelf

441 attributed to the damming of the Nile River, The Israeli Ministry of National Infrastructure, Energy and

442 Water Resources, Report ES-30-2009, 2009.

443 Antler, G., Turchyn, A. V., Herut, B., Sivan, O.: A unique isotopic fingerprint of sulfate-driven

444 anaerobic oxidation of methane. Geology., 43, 619–622, 2015.

445 Astrahan, P., Silverman, J., Gertner, Y. and Herut, B.: Spatial distribution and sources of organic

446 matter and pollutants in the SE Mediterranean (Levantine basin) deep water sediments, Mar. Pollut.

447 Bull., 116(1–2), 521–527, doi:10.1016/j.marpolbul.2017.01.006, 2017.

448 Bar-Or, I., Ben-Dov, E., Kushmaro, A., Eckert, W. and Sivan, O.: Methane-related changes in

449 prokaryotes along geochemical profiles in sediments of Lake Kinneret (Israel), Biogeosciences, 12,

450 2847–2860, doi:10.5194/bg-12-2847-2015, 2015.

451 Bar-Or, I., Elvert, M., Eckert, W., Kushmaro, A., Vigderovich, H., Zhu, Q., Ben-Dov, E. and Sivan, O.:

452 Iron-Coupled Anaerobic Oxidation of Methane Performed by a Mixed Bacterial-Archaeal Community

453 Based on Poorly Reactive Minerals, Environ. Sci. Technol., 51, 12293-12301

454 doi:10.1021/acs.est.7b03126, 2017.

455   Beal, E. J., House, C. H. and Orphan, V. J.: Manganese-and Iron-Dependent Marine Methane

456   Oxidation, Science, 325(5937), 184–187, 10.1126/science.1169984, 2009.

457   Bond, D. R., Lovley, D. R. and Methanococcus, A.: Reduction of Fe (III) oxide by methanogens in

458   the presence and absence of extracellular quinones, Environ. Microbiol., 4(2), 115–124,

459   10.1046/j.1462-2920.2002.00279.x, 2002.

460   Bond, P. L., Hugenholtz, P., Keller, J. and Blackall, L. L.: Bacterial Community Structures of

461   Phosphate-Removing and Non-Phosphate-Removing Activated Sludges from Sequencing Batch

462   Reactors, , 61(5), 1910–1916, https://aem.asm.org/content/61/5/1910.short, 1995.

463   Bottrell, S. H., Parkes, R. J., Cragg, B. a. and Raiswell, R.: Isotopic evidence for anoxic pyrite

464   oxidation and stimulation of bacterial sulphate reduction in marine sediments, J. Geol. Soc. London.,

465   157(4), 711–714, doi:10.1144/jgs.157.4.711, 2000.

466   Buongiorno, J., Turner, S., Webster, G., Asai, M., Shumaker, A. K., Roy, T., Weightman, A.,

467   Schippers, A. and Lloyd, K. G.: Interlaboratory quantification of Bacteria and Archaea in deeply buried

468   sediments of the Baltic Sea (IODP Expedition 347), FEMS Microbiol. Ecol., (93), 1–16,

469   doi:10.1093/femsec/fix007, 2017.

470   Burdige, D. J, and Komada, T.,: Anaerobic oxidationof methane and the stoichiometry of

471   remineralization processes in continental margin sediments, Limnol. Oceanogr., 56(5), 1781-1796, doi:

472   10.4319/lo.2011.56.5.1781, 2011.

473   Cai, C., Leu, A. O., Jianhua, G. X., Yuexing, G., Zhao, F. J. and Tyson, G. W.: A methanotrophic

474   archaeon couples anaerobic oxidation of methane to Fe (III) reduction, ISME J., (Iii),

475   doi:10.1038/s41396-018-0109-x, 2018.

476   Chen, W. H., Chen, S. Y., Kumar Khanal, S. and Sung, S.: Kinetic study of biological hydrogen

477   production by anaerobic fermentation, Int. J. Hydrogen Energy, 31(15), 2170–2178,

478   doi:10.4304/jcp.6.4.740-746, 2006.

479   Cline, J. D.: Spectrophotometric determination of hydrogen sulfide in natural waters, Limnol.

480   Oceanogr., 454–458, https://doi.org/10.4319/lo.1969.14.3.0454, 1969.

481   Conrad, R.: Contribution of hydrogen to methane production and control of hydrogen concentrations in

482   methanogenic soils and sediments, FEMS Microbiol. Ecol., 28(3), 193–202,

483   https://doi.org/10.1111/j.1574-6941.1999.tb00575.x, 1999.

484   Coolen, M. J. L., Cypionka, H., Sass, A. M., Sass, H. and Overmann, J.: Ongoing modification of

485   Mediterranean pleistocene sapropels sediated by prokaryotes, Science., 296, 2407–2411,

486   10.1126/science.1071893, 2002.

487   Crowe, S. A., Katsev, S., Leslie, K., Sturm, A., Magen, C., Nomosatryo, S., Pack, M. A., Kessler, J. D.,

488   Reeburgh, W. S., Robert S J, A., Gonzalez, L., Douglas Haffner, G., Mucci, A., Sundby, B. and Fowle,

489   D. .: The methane cycle in ferruginous Lake Matano, Geobiology, 9, 61–78, doi:10.1111/j.1472-

490   4669.2010.00257.x, 2011.

491   Egger, M., Rasigraf, O., Sapart, C. J., Jilbert, T., Jetten, M. S. M., Röckmann, T., Van Der Veen, C.,

492   Bânda, N., Kartal, B., Ettwig, K. F. and Slomp, C. P.: Iron-mediated anaerobic oxidation of methane in

493   brackish coastal sediments, Environ. Sci. Technol., 49(1), 277–283, doi:10.1021/es503663z, 2015.

494   Egger, M., Kraal, P., Jilbert, T., Sulu-Gambari, F., Sapart, C. J., Röckmann, T. and Slomp, C. P.:

495   Anaerobic oxidation of methane alters diagenetic records of sulfur, iron and phosphorus in Black Sea

496   sediments, Biogeosciences Discuss., 1–39, doi:10.5194/bg-2016-64, 2016.

497   Ettwig, K. F., Zhu, B., Speth, D., Keltjens, J. T., Jetten, M. S. M. and Kartal, B.: Archaea catalyze iron-

498   dependent anaerobic oxidation of methane, Proc. Natl. Acad. Sci., 113(45), 12792–12796,

499   doi:10.1073/pnas.1609534113, 2016.

500   Evans, P. N., Parks, D. H., Chadwick, G. L., Robbins, S. J., Orphan, V. J., Golding, S. D. and Tyson,

501   G. W.: Methane metabolism in the archaeal phylum Bathyarchaeota revealed by genome-centric

502   metagenomics, Science., 350(6259), 434–438, doi:10.1126/science.aac7745, 2015.

503   Feng, X., Wang, Y., Zubin, R. and Wang. F., Core metabolic features and hot origin of Bathyarchaeota.

504   Engineering. Accepted.

505   Froelich, P. N., Klinkhammer, G. P., Bender, M. L., Luedtke, N. A., Heath, G. R., Cullen, D., Dauphin,

506   P., Hammond, D., Hartman, B. and Maynard, V.: Early oxidation of organic matter in pelagic

507   sediments of the eastern equatorial Atlantic: Suboxic diagenesis, Geochim. Cosmochim. Acta, 43,

508   1075–1090, https://doi.org/10.1016/0016-7037(79)90095-4, 1979.

509   He, Y., Li, M., Perumal, V., Feng, X., Fang, J., Xie, J., Sievert, S. M. and Wang, F.: Genomic and

510   enzymatic evidence for acetogenesis among multiple lineages of the archaeal phylum Bathyarchaeota

511   widespread in marine sediments, Nat. Microbiol., 1–9, doi:10.1038/nmicrobiol.2016.35, 2016.

512   Herut, B., Almogi-Labin, A., Jannink, N. and Gertman, I.: The seasonal dynamics of nutrient and

513   chlorophyll a concentrations on the SE Mediterranean shelf-slope, Oceanol. Acta, 23, 771–782,

514   doi:10.1016/S0399-1784(00)01118-X, 2000.

515   Hoehler, T. M., Alperin, M. J., Albert, D. B. and Martens, C. S.: Field and laboratory studies of

516   methane oxidation in an anoxic marine sediment: evidence for a methanogen-sulfate reducer

517   consortium, Global Biogeochem. Cycles, 8(4), 451–463, https://doi.org/10.1029/94GB01800, 1994.

518   Holmkvist, L., Ferdelman, T. G. and Jørgensen, B. B.: A cryptic sulfur cycle driven by iron in the

519   methane zone of marine sediment (Aarhus Bay, Denmark), Geochim. Cosmochim. Acta, 75(12), 3581–

520   3599, doi:10.1016/j.gca.2011.03.033, 2011.

521   Caporaso, J. G., Kuczynski, J., Stombaugh, J., Bittinger, K., Bushman, F. D., Costello, E. K., Fierer,

522   N., Peña, A. G., Goodrich, J. K., Gordon, J. I., Huttley, G. A., Kelley, S. T., Knights, D., Koenig, J. E.,

523   Ley, R. E., Lozupone, C. A., McDonald, D., Muegge, B. D., Pirrung, M., Reeder, J., Sevinsky, J. R.,

524   Turnbaugh, P. J., Walters, W. A., Widmann, J., Yatsunenko, T., Zaneveld, J., and Knight, R.: QIIME

allows analysis of high-throughput com- munity sequencing data., Nat. Methods, (7), 335–336, doi: 10.1038/nmeth.f.303, 2010.

Jorgensen, B. B., Bottcher, M. E., Luschen, H., Neretin, L. N. and Volkov, I. I.: Anaerobic methane oxidation and a deep H 2 S sink generate isotopically heavy sulfides in Black Sea sediments, Geochim. Cosmochim. Acta, 68(9), 2095–2118, doi:10.1016/j.gca.2003.07.017, 2004.

Kappler, A. and Straub, K. L.: Geomicrobiological Cycling of Iron, Rev. Mineral. Geochemistry, 59(II), 85–108, doi:10.2138/rmg.2005.59.5, 2005.

Kawaichi, S., Ito, N., Kamikawa, R., Sugawara, T., Yoshida, T. and Sako, Y.: Ardenticatena maritima gen. nov., sp. nov., a ferric iron- and nitrate-reducing bacterium of the phylum 'Chloroflexi' isolated from an iron-rich coastal hydrothermal field, and description of Ardenticatenia classis nov., Int. J. Syst. Evol. Microbiol., (63), 2992–3002, doi:10.1099/ijs.0.046532-0, 2013.

Kress, N. and Herut, B.: Spatial and seasonal evolution of dissolved oxygen and nutrients in the Southern Levantine Basin (Eastern Mediterranean Sea): chemical characterization of the water masses and inferences on the N : P ratios, , 48, 2347–2372, doi:10.1016/S0967-0637(01)00022-X, 2001.

Kulichevskaya, I. S., Suzina, N. E., Rijpstra, W. I. C., Dedysh, S. N. and Damste, J. S. S.: a facultative anaerobe capable of dissimilatory iron reduction from subdivision 3 of the Acidobacteria, Int. J. Syst. Evol. Microbiol., (64), 2857–2864, doi:10.1099/ijs.0.066175-0, 2014.

Li, Y., Yu, S., Strong, J. and Wang, H.: Are the biogeochemical cycles of carbon , nitrogen , sulfur , and phosphorus driven by the " Fe III – Fe II redox wheel " in dynamic redox environments?, J. Soils sediemnts, 12(5), 683–693, doi:10.1007/s11368-012-0507-z, 2012.

Lilley, M. D., Baross, J. A. and Gordon, L. I.: Dissolved hydrogen and methane in Saanich Inlet, British Columbia, Deep Sea Res. Part A, Oceanogr. Res. Pap., 29(12), 1471–1484, doi:10.1016/0198-0149(82)90037-1, 1982.

Liu, D., Dong Hailiang, H., Bishop, M. E., Wang, H., Agrawal, A., Tritschler, S., Eberl, D. D. and Xie, S.: Reduction of structural Fe(III) in nontronite by methanogen Methanosarcina barkeri, Geochim. Cosmochim. Acta, 75(4), 1057–1071, doi:10.1016/j.gca.2010.11.009, 2011.

Lloyd, K. G., Schreiber, L., Petersen, D. G., Kjeldsen, K. U., Lever, M. A., Steen, A. D., Stepanauskas, R., Richter, M., Kleindienst, S., Lenk, S., Schramm, A. and Jørgensen, B. B.: Predominant archaea in marine sediments degrade detrital proteins, Nature, 496(7444), 215–218, doi:10.1038/nature12033, 2013.

Lovley, Derek R. and Goodwin, S.: Hydrogen concentrations as an indicator of the predominant terminal electron-accepting reactions in aquatic sediments, 52, 2993-3003, doi: 10.1016/0016-7037(88)90163-9, 1988.

Lovley, D. R.: Dissimilatory Fe(III) and Mn(IV) reduction., Microbiol. Rev., 55(2), 259–287, 1991.

Lovley, D. R. and Phillips, E. J.: Novel mode of microbial energy metabolism: organic carbon

560   oxidation coupled to dissimilatory reduction of iron or manganese., Appl. Environ. Microbiol., 54(6),

561   1472–1480, doi:10.1103/PhysRevLett.50.1998, 1988.

562   Lovley, D. R. and Phillips, E. J. P.: Organic matter mineralization with reduction of ferric iron in

563   anaerobic sediments., Appl. Environ. Microbiol., 51(4), 683–689, doi:10.1080/01490458709385975,

564   1986.

565   Lovley, D. R., Coates, J. D., BluntHarris, E. L., Phillips, E. J. P. and Woodward, J. C.: Humic

566   substances as electron acceptors for microbial respiration, Nature, 382(6590), 445–448,

567   doi:10.1038/382445a0, 1996.

568   März, C., Hoffmann, J., Bleil, U., Lange, G. J. De and Kasten, S.: Diagenetic changes of magnetic and

569   geochemical signals by anaerobic methane oxidation in sediments of the Zambezi deep-sea fan (SW

570   Indian Ocean), Mar. Geol., 255(3–4), 118–130, doi:10.1016/j.margeo.2008.05.013, 2008.

571   McGlynn, S. E., Chadwick, G. L., Kempes, C. P. and Orphan, V. J.: Single cell activity reveals direct

572   electron transfer in methanotrophic consortia, Nature, 526(7574), 531–535, doi:10.1038/nature15512,

573   2015.

574   Meng, J., Xu, J., Qin, D., He, Y., Xiao, X. and Wang, F.: Genetic and functional properties of

575   uncultivated MCG archaea assessed by metagenome and gene expression analyses, ISME J., 8(3), 650–

576   9, doi:10.1038/ismej.2013.174, 2014.

577   Mountfort, D. O. and Asher, R. A.: Role of Sulfate Reduction Versus Methanogenesis in Terminal

578   Carbon Flow in Polluted Intertidal Sediment of Waimea Inlet, Nelson, New Zealand, Appl. Environ.

579   Microbiol., 42(2), 252–258, http://aem.asm.org/cgi/reprint/42/2/252, 1981.

580   Mountfort, D. O., Asher, R. a, Mays, E. L. and Tiedje, J. M.: Carbon and electron flow in mud and

581   sandflat intertidal sediments at delaware inlet, nelson, new zealand., Appl. Environ. Microbiol., 39(4),

582   686–94, http://aem.asm.org/content/39/4/686, 1980.

583   Nir, Y.: Recent sediments of the Israel Mediterranean continental shelf and slope, Ph.D. thesis,

584   University of Gothenburg, Sweden, 1984.

585   Niu, M., Fan, X., Zhuang, G., Liang, Q. and Wang, F.: Methane-metabolizing microbial communities

586   in sediments of the Haima cold seep area , northwest slope of the South China Sea, FEMS Microbiol.

587   Ecol., 1–13, doi:10.1093/femsec/fix101, 2017.

588   Norði, K. Á. and Thamdrup, B.: Nitrate-dependent anaerobic methane oxidation in a freshwater

589   sediment, Geochim. Cosmochim. Acta, 132, 141–150, doi:10.1016/j.gca.2014.01.032, 2014.

590   Novelli, P. C., Scranton, M. I. and Michener, R. H.: Hydrogen Distributions in Marine Sediments

591   Hydrogen distributions, , 32(3), 565–576, doi: 10.4319/lo.1987.32.3.0565, 1987.

592   Nusslein, B., Eckert, W. and Conrad, R.: Stable isotope biogeochemistry of methane formation in

593   profundal sediments of Lake Kinneret (Israel), 48(4), 1439–1446, doi: 10.4319/lo.2003.48.4.1439,

594   2003.

595 Oni, O., Miyatake, T., Kasten, S., Richter-Heitmann, T., Fischer, D., Wagenknecht, Laura Kulkarni, A.,
596 Blumers, M., Shylin, S. I., Ksenofontov, Vadim Costa, B. F. O., Klingelhöfer, G. and Friedrich, M. W.:
597 Distinct microbial populations are tightly linked to the profile of dissolved iron in the methanic
598 sediments of the Helgoland mud area, North Sea, Front. Microbiol., 6, 1–15,
599 doi:10.3389/fmicb.2015.00365, 2015.

600 Poulton, S. W. and Canfield, D. E.: Development of a sequential extraction procedure for iron:
601 Implications for iron partitioning in continentally derived particulates, Chem. Geol., 214(3–4), 209–
602 221, doi:10.1016/j.chemgeo.2004.09.003, 2005.

603 Riedinger, N., Formolo, M. J., Lyons, T. W., Henkel, S., Beck, A. and Kasten, S.: An inorganic
604 geochemical argument for coupled anaerobic oxidation of methane and iron reduction in marine
605 sediments, Geobiology, 12(2), 172–181, doi:10.1111/gbi.12077, 2014.

606 Roden, E. E.: Fe(III) oxide reactivity toward biological versus chemical reduction, Environ. Sci.
607 Technol., 37(7), 1319–1324, doi: 10.1021/es026038o, 2003.

608 Roden, E. E.: Geochemical and microbiological controls on dissimilatory iron reduction, Comptes
609 Rendus - Geosci., 338(6–7), 456–467, doi:10.1016/j.crte.2006.04.009, 2006.

610 Roden, E. E. and Wetzel, R. G.: Organic carbon oxidation and suppression of methane production by
611 microbial Fe(III) oxide reduction in vegetated and unvegetated freshwater wetland sediments, Limnol.
612 Oceanogr., 41(8), 1733–1748, doi: 10.4319/lo.1996.41.8.1733, 1996.

613 Roden, E. E. and Wetzel, R. G.: Kinetics of microbial Fe (III) oxide reduction in freshwater wetland
614 sediments, Limnol. Ocean., 47(1), 198–211, doi: 10.4319/lo.2002.47.1.0198, 2002.

615 Rooze, J., Egger, M., Tsandev, I. and Slomp, C. P.: Iron-dependent anaerobic oxidation of methane in
616 coastal surface sediments: potential controls and impact, Limnol. Oceanogr., (1),
617 doi:10.1002/lno.10275, 2016.

618 Rotaru, B. A. and Thamdrup, B.: A new diet for methane oxidizers, Biogeochemistry, 351(6274), 658–
619 660, doi: 10.1126/science.aaf0741, 2016.

620 Salem, D. M. S. A., Khaled, A. and Nemr, A. El: Assessment of pesticides and polychlorinated
621 biphenyls (PCBs) in sediments of the Egyptian Mediterranean Coast, Egypt. J. Aquat. Res., 39(3),
622 141–152, doi:10.1016/j.ejar.2013.11.001, 2013.

623 Sandler, A. and Herut, B.: Composition of clays along the continental shelf off Israel: Contribution of
624 the Nile versus local sources, Mar. Geol., 167(3–4), 339–354, doi:10.1016/S0025-3227(00)00021-9,
625 2000.

626 Schattner, U., Lazar, M., Harari, D. and Waldmann, N.: Active gas migration systems offshore northern
627 Israel, first evidence from seafloor and subsurface data, Cont. Shelf Res., 48, 167–172,
628 doi:10.1016/j.csr.2012.08.003, 2012.

629 Scheller, S., Yu, H., Chadwick, G. L., McGlynn, S. E. and Orphan, V. J.: Artificial electron acceptors

630 decouple archaeal methane oxidation from sulfate reduction, Science., 351(6274), 1754–1756,

631 doi:10.1126/science.aad7154, 2016.

632 Segarra, K. E. a, Comerford, C., Slaughter, J. and Joye, S. B.: Impact of electron acceptor availability

633 on the anaerobic oxidation of methane in coastal freshwater and brackish wetland sediments, Geochim.

634 Cosmochim. Acta, 115, 15–30, doi:10.1016/j.gca.2013.03.029, 2013.

635 Sela-Adler, M., Herut, B., Bar-Or, I., Antler, G., Eliani-Russak, E., Levy, E., Makovsky, Y. and Sivan,

636 O.: Geochemical evidence for biogenic methane production and consumption in the shallow sediments

637 of the SE Mediterranean shelf (Israel), Cont. Shelf Res., 101, 117–124, doi:10.1016/j.csr.2015.04.001,

638 2015.

639 Sivan, O., Schrag, D. P. and Murray, R. W.: Rates of methanogenesis and methanotrophy in deep-sea

640 sediments, Geobiology, 5(2), 141–151, doi:10.1111/j.1472-4669.2007.00098.x, 2007.

641 Sivan, O., Adler, M., Pearson, A., Gelman, F., Bar-Or, I., John, S. G. and Eckert, W.: Geochemical

642 evidence for iron-mediated anaerobic oxidation of methane, Limnol. Oceanogr., 56(4), 1536–1544,

643 doi:10.4319/lo.2011.56.4.1536, 2011.

644 Sivan, O., Antler, G., Turchyn, A. V., Marlow, J. J. and Orphan, V. J.: Iron oxides stimulate sulfate-

645 driven anaerobic methane oxidation in seeps, Proc. Natl. Acad. Sci., 111, E4139–E4147,

646 doi:10.1073/pnas.1412269111, 2014.

647 Sivan, O., Shusta, S. and Valentine, D. L.: Methanogens rapidly transition from methane production to

648 iron reduction, Geobiology, 190–203, doi:10.1111/gbi.12172, 2016.

649 Slomp, C. P., Mort, H. P., Jilbert, T., Reed, D. C., Gustafsson, B. G. and Wolthers, M.: Coupled

650 Dynamics of Iron and Phosphorus in Sediments of an Oligotrophic Coastal Basin and the Impact of

651 Anaerobic Oxidation of Methane, PLoS One, 8(4), doi:10.1371/journal.pone.0062386, 2013.

652 Song, Z., Wang, F., Zhi, X., Chen, J., Zhou, E., Liang, F., Xiao, X., Tang, S., Jiang, H., Zhang, C. L.,

653 Dong, H. and Li, W.: Bacterial and archaeal diversities in Yunnan and Tibetan hot springs , China, , 15,

654 1160–1175, doi:10.1111/1462-2920.12025, 2013.

655 Stookey, L. L.: Ferrozine-a new spectrophotometric reagent for iron, Anal. Chem., 42(7), 779–781,

656 doi:10.1021/ac60289a016, 1970.

657 Treude, T., Krause, S., Maltby, J., Dale, A. W., Coffin, R. and Hamdan, L. J.: Sulfate reduction and

658 methane oxidation activity below the sulfate-methane transition zone in Alaskan Beaufort Sea

659 continental margin sediments: Implications for deep sulfur cycling, Geochim. Cosmochim. Acta, 144,

660 217–237, doi:10.1016/j.gca.2014.08.018, 2014.

661 Walters, W., Hyde, E. R., Berg-lyons, D., Ackermann, G., Humphrey, G., Parada, A., Gilbert, J. A. and

662 Jansson, J. K.: Transcribed Spacer Marker Gene Primers for Microbial Community Surveys, Am. Soc.

663 Microbiol., 1(1), 1–10, doi:10.1128/mSystems.00009-15.Editor, 2015.

664 Wang, Z., Guo, F., Liu, L. and Zhang, T.: Evidence of Carbon Fixation Pathway in a Bacterium from

665   Candidate Phylum SBR1093 Revealed with Genomic Analysis, PLoS One, 9(10),

666   doi:10.1371/journal.pone.0109571, 2014.

667   Weber, K. A., Urrutia, M. M., Churchill, P. F., Kukkadapu, R. K. and Roden, E. E.: Anaerobic redox

668   cycling of iron by freshwater sediment microorganisms, Environ. Microbiol., 8(1), 100–113,

669   doi:10.1111/j.1462-2920.2005.00873.x, 2006.

670   Whiticar, M. J.: Carbon and hydrogen isotope systematics of bacterial formation and oxidation of

671   methane, Chem. Geol., 161(1–3), 291–314, doi:10.1016/S0009-2541(99)00092-3, 1999.

672   Yan, Z., Joshi, P., Gorski, C. A. and Ferry, J. G.: A biochemical framework for anaerobic oxidation of

673   methane driven by Fe(III)-dependent respiration, Nat. Commun., 1–9, doi:10.1038/s41467-018-04097-

674   9, 2018.

675   Yu, T., Wu, W., Liang, W., Alexander, M. and Hinrichs, K.: Growth of sedimentary Bathyarchaeota on

676   lignin as an energy source, Proc. Natl. Acad. Sci., 115(23), 6022–6027, doi:10.1073/pnas.1718854115,

677   2018.

678   Zehnder, a. J. B. and Brock, T. D.: Anaerobic methane oxidation: Occurrence and ecology, Appl.

679   Environ. Microbiol., 39(1), 194–204, 1980.

680   Zhang, J., Dong, H., Liu, D., Fischer, T. B., Wang, S. and Huang, L.: Microbial reduction of Fe(III) in

681   illite–smectite minerals by methanogen Methanosarcina mazei, Chem. Geol., 292–293, 35–44, 2012.

682   Zhang, J., Dong, H., Liu, D. and Agrawal, A.: Microbial reduction of Fe(III) in smectite minerals by

683   thermophilic methanogen Methanothermobacter thermautotrophicus, Geochim. Cosmochim. Acta,

684   106(Iii), 203–215, doi: 10.1016/j.gca.2012.12.031, doi: 10.1016/j.chemgeo.2011.11.003, 2013.

685   Zhou, Z., Pan, J., Wang, F., Gu, J. and Li, M.: Bathyarchaeota : globally distributed metabolic

686   generalists in anoxic environments, FEMS Microbiol. Rev., (May), 639–655,

687   doi:10.1093/femsre/fuy023, 2018.

688

689

690   **Figures captions:**

Figure 1: Geochemical pore-water profiles of sediment cores collected from the three stations SG-1 (top), PC-3 (middle) and PC-5 (bottom) in the Eastern Mediterranean. The profiles are divided roughly to three zones according to the dominant processes: upper microbial iron and sulfate reduction, sulfate-methane transition zone (SMTZ), and the methanogenic zone at the deep part. The dashed line in the CH_4 graph at SG-1 station represents the CH_4 saturation value in the pore-water. The error bars for CH_4 are presented where duplicate sediment samples were collected. The error bars for Fe(II), $\delta^{13}C_{DIC}$ and H_2 are presented where measurement repetition of each sample was taken (at least twice). The analytical errors were smaller than the symbols.

Figure 2: Sedimentary depth profiles of bacterial and archaeal 16S rRNA and mcrA functional genes of Station SG-1 from January 2017. Triplicates were made for each sample with error bars smaller than the symbols.

Figure 3: Phyla level classification of bacterial (a) and archaeal (b) diversity in the sediments of Station SG-1 from January 2017.

Figure 4: Dissolved Fe(II) results of the sediment slurry incubation experiment from SG-1 core. The sediment was collected on January 2017 from sediment depth of 260 cm. The error bars were smaller than the symbol.

Figure 5: The relationship between dissolved Fe(II) concentrations and methane concentrations in zone 3 sediments at (a) Station SG-1 and (b) Station PC-3. An inverse association is observed between the two species, suggesting a relationship of competition or Fe(III)-coupled anaerobic methane oxidation.

691

692   **Figures**:

693   **Figure 1**
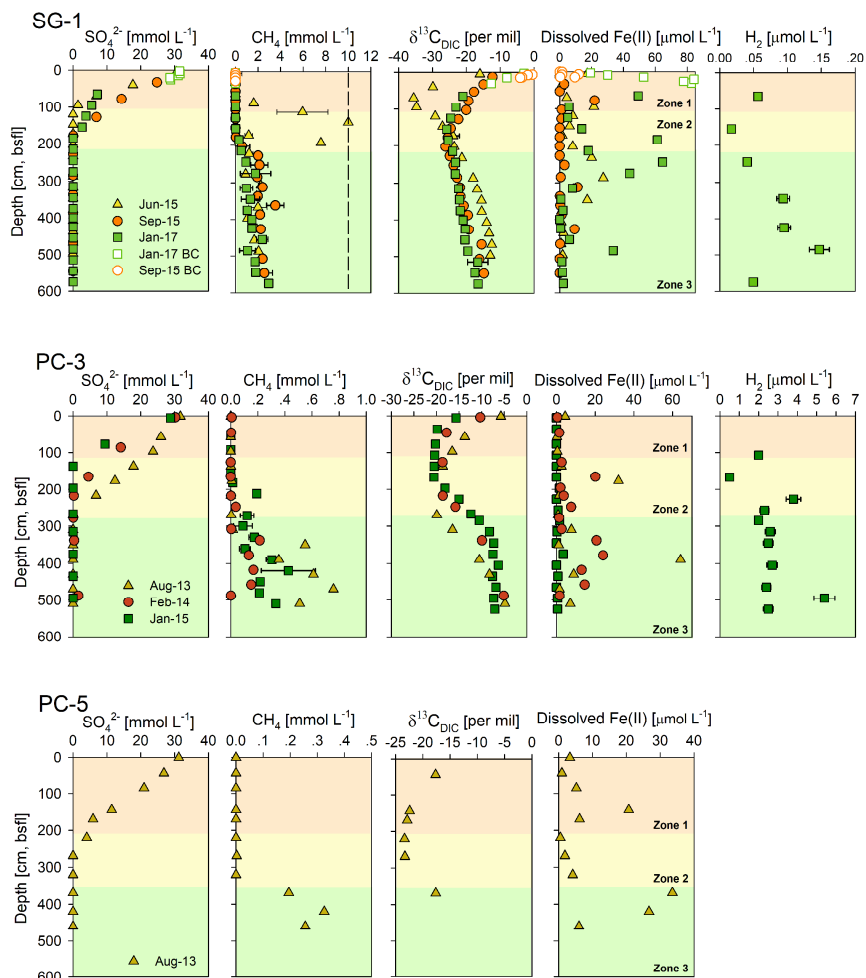
694

695

696   **Figure 2**
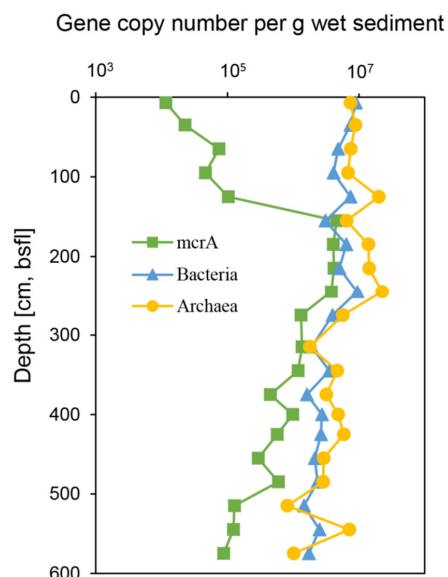
697

698

699   **Figure 3**
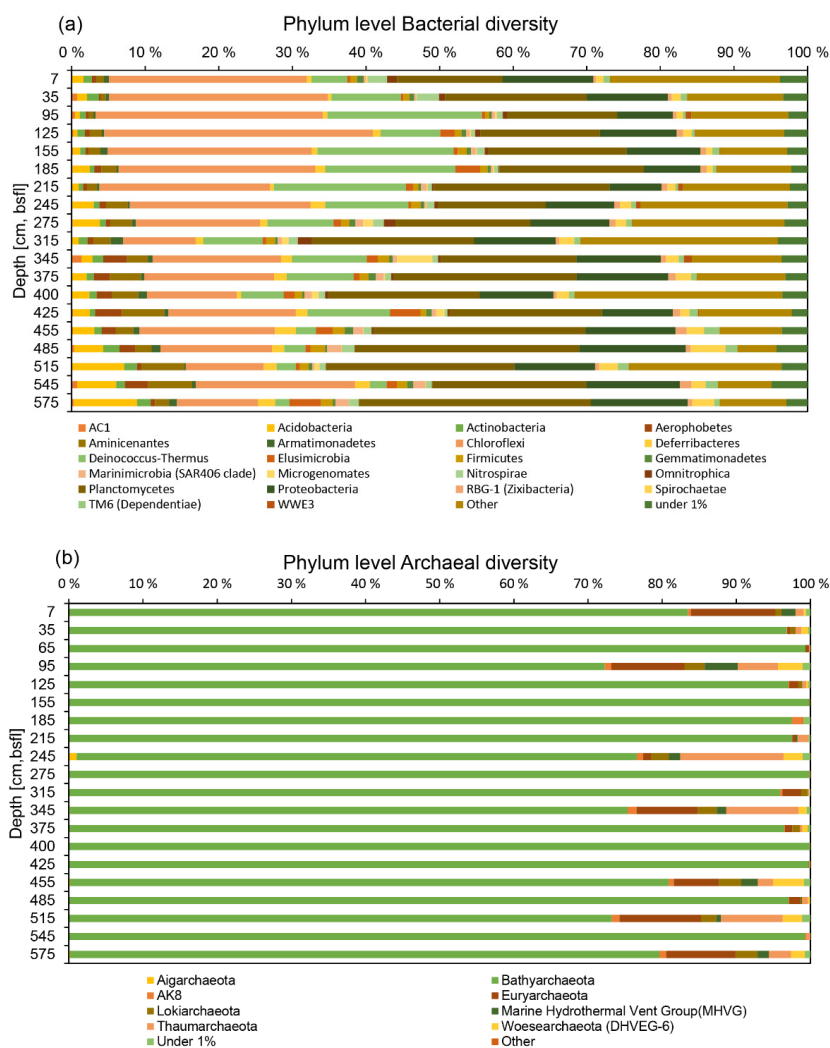
700

701

702 **Figure 4**
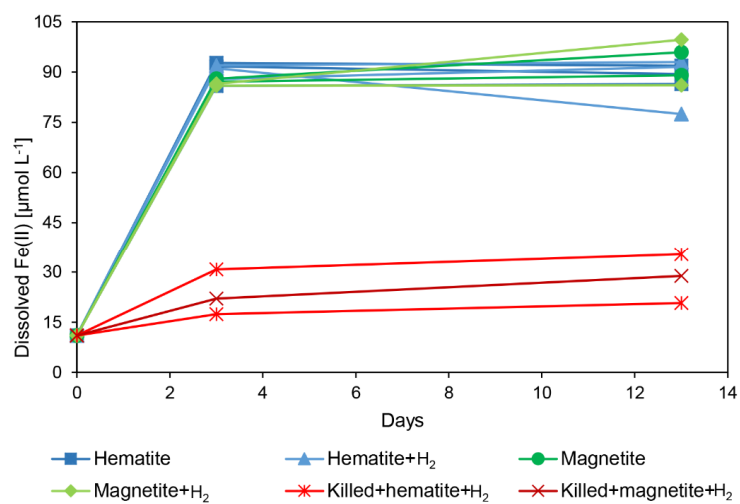
703

704

705   **Figure 5**
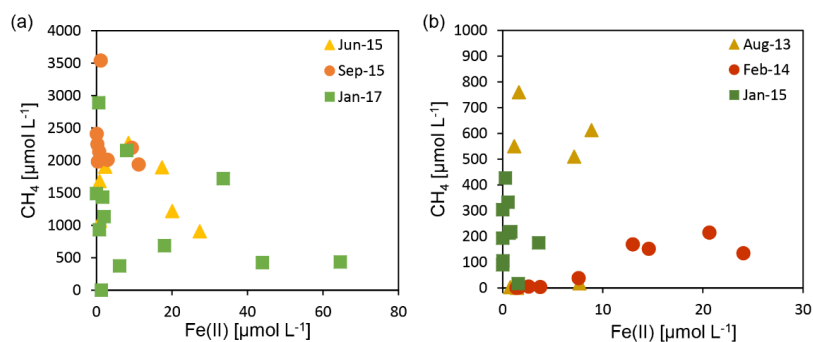
706

707

708

709

710

711

712

713